

The absolute value of the quantum yield of the fluorescence of the ${}^1B_{3u}$ 0-0 state of pyrazine as a function of the rotational quantum numbers

Pieter J. de Lange, Barend J. van der Meer, Karel E. Drabe,^{a)} and Jan Kommandeur
Laboratory for Physical Chemistry, University of Groningen, Nijenborgh 16, 9747 AG Groningen, The Netherlands

W. Leo Meerts and W. A. Majewski^{b)}
Fysisch Laboratorium, Katholieke Universiteit Nijmegen, Toernooiveld, 6525 ED Nijmegen, The Netherlands

(Received 14 October 1986; accepted 16 December 1986)

In this paper we fit low-resolution spectra of pyrazine by assuming Coriolis coupling between S_1 and $\{S_0\}$. Evidence for Coriolis coupling is particularly obvious in the rovibronic spectra of pyrazine- d_3h_1 of which we give high resolution examples. For the lowest rotational temperature we noticed a non-Boltzmann distribution of the $J'' = 0$ ground state, which is probably caused by a bottleneck for $\Delta J'' = -2$ transitions. Using the lifetimes of molecular eigenstates belonging to $P(1)$ we can calculate the absolute quantum yield of the vibrationless and rotationless ${}^1B_{3u}$ state. Using this number and the obtained interstate Coriolis coupling rate constants we calculate the variation of the absolute quantum yield across the rotational contour. For low J we get satisfactory agreement with experiments, but for high J our calculations drop off too fast with J . We explain this by the fact that at high J values triplet decay becomes dominant because of K scrambling in the triplet manifold.

I. INTRODUCTION

The electronic decay of the ${}^1B_{3u}$ (0-0) state of pyrazine has in recent years yielded many of its secrets through intensive studies. Quantum beats were observed,^{1,2} the molecular eigenstate (ME) spectrum is known in great detail^{3,4} and it has recently become possible to find the energies of the zero order states and the coupling elements between them.^{5,6}

A problem still remains with the value of the quantum yield and with the nature of the interactions observed. Very recently Amirav and Jortner⁷ showed that the quantum yield is high for low J 's and decreases as $(2J' + 1)^{-1}$, a conclusion that was arrived at on the basis of more qualitative observations by Baba *et al.*^{8,9} In principle, this effect was explained in Ref. 7 where it was proposed that the number of coupled triplet states increased with J' . However, for low J' values, this is in contrast with what is found from the ME spectra, where the number of coupled triplets appears to be independent of J' .⁵

We therefore decided to investigate accurately the intensities of the low J excitation spectrum of the ${}^1B_{3u}$ ground vibrational state of pyrazine in order to obtain relative quantum yield values and possibly to gain more information about the mechanisms for the radiationless decay of S_1 and T . Elsewhere,⁴ we will report a study of the lifetimes of a number of ME's belonging to the $J' = 0, K' = 0$ state. From these lifetimes, which vary from 200 to 560 ns it can be concluded unequivocally that both the triplet and the singlet character of an ME play a role in this decay. We will see on the basis of the present results that for higher J' values the triplet decay becomes dominant.

^{a)} Present address: Laboratory for Physical Chemistry, University of Amsterdam, Nieuwe Achtergracht 127, 1018 WS Amsterdam, The Netherlands.

^{b)} Present address: Department of Chemistry, University of Pittsburgh, Pittsburgh, Pennsylvania 15260.

II. EXPERIMENTAL

A. Low resolution measurements

The molecular beam apparatus consists of a pulsed nozzle (1 mm diameter) mounted in a vacuum chamber. The system was pumped by an 18B3A Edwards oil booster pump (pumping speed 1200 ℓ/s), backed by an Edwards ES4000 rotary pump.

Excitation was provided by a Nitrogen pumped dye laser (Moletron UV1000 + Lambda Physik 2001E). The dye laser was equipped with an intracavity étalon, and tuned by changing pressure. Excitation bandwidth (before frequency doubling) is ~ 1 GHz, and pulse duration ~ 4 ns. Pyrazine is seeded in He. The precise backing pressures are given in Table I. All excitation spectra were taken with a boxcar integrator with a 1 μs gate placed 50 ns after the laser pulse, thus excluding the contribution of the fast component to the excitation spectra. Further data acquisition was facilitated by an Apple IIe computer. In this way the individual peaks could be integrated, and expressed as a fraction of the total intensity. The accuracy of these determinations is estimated to be about 10% of this fraction. The results are given in Table I (column expt) for four different backing pressures. The spectrum at the highest backing pressure (T_1) is displayed in Fig. 1(a). Note that the peaks all have different widths. The smallest linewidth occurs for $R(1)$, and the lines broaden for higher J'' .

B. High resolution measurements

The apparatus situated at Nijmegen has been described in detail before,^{10,11} hence only the most relevant features are discussed here. A collimated molecular beam was crossed at right angles by a cw single frequency tunable UV laser beam. The molecular beam was formed by expanding a mixture of saturated pyrazine vapor and argon through a 100 μm nozzle.

TABLE I. Calculated and measured intensities of rotational transitions.

	T_1				T_2				T_3			T_4		
	Symm top ^a	Cor ^b	Cor $N-B^c$	Expt	Symm top ^a	Cor ^b	Cor $N-B^c$	Expt	Symm top ^a	Cor ^b	Expt	Symm top ^a	Cor ^b	Expt
$R(8)$												0.064	0.037	0.043
$R(7)$									0.027	0.027	0.033	0.080	0.044	0.061
$R(6)$									0.057	0.044	0.038	0.101	0.055	0.060
$R(5)$									0.091	0.057	0.067	0.101	0.058	0.083
$R(4)$					0.022	0.010	0.008	0.020	0.141	0.081	0.067	0.106	0.069	0.074
$R(3)$	0.015	0.015	0.017	0.014	0.071	0.042	0.031	0.038	0.143	0.085	0.067	0.078	0.063	0.065
$R(2)$	0.119	0.081	0.076	0.067	0.173	0.098	0.103	0.083	0.144	0.100	0.087	0.061	0.067	0.057
$R(1)$	0.253	0.155	0.182	0.201	0.147	0.097	0.123	0.158	0.065	0.062	0.108	0.023	0.038	0.052
$R(0)$	0.194	0.148	0.126	0.128	0.077	0.068	0.052	0.061	0.025	0.035	0.038	0.008	0.021	0.021
Q	0.339	0.442	0.467	0.430	0.384	0.447	0.472	0.410			d			d
$P(1)$	0.038	0.061	0.070	0.067	0.024	0.041	0.051	0.057	0.011	0.027	0.070	0.004	0.017	...
$P(2)$	0.036	0.083	0.067	0.080	0.065	0.116	0.114	0.097	0.060	0.129	0.145	0.026	0.087	0.113
$P(3)$	0.004	0.015	0.007	0.012	0.030	0.056	0.038	0.044	0.074	0.127	0.103	0.041	0.096	0.099
$P(4)$					0.009	0.019	0.008	0.023	0.082	0.116	0.094	0.065	0.102	0.091
$P(5)$									0.056	0.079	0.073	0.067	0.083	0.082
$P(6)$									0.035	0.056	0.053	0.070	0.074	0.070
$P(7)$												0.057	0.057	0.057
$P(8)$												0.046	0.047	0.049
p^c				2 bar				1 bar			0.5 bar			0.2 bar
T^f	0.55 K	0.8 K	0.6 K		1.1 K	1.7 K	1.2 K		3.5 K	8 K		8 K	18 K	
x^g	0.3		0.1		
σ^h	0.051	0.020	0.014		0.034	0.025	0.022		0.045	0.018		0.033	0.012	

^aSymmetrical top application only.^bSymmetrical top and Coriolis.^cSymmetrical top, Coriolis, and non-Boltzmann distribution.^dFor high T the Q -branch intensity was not included.^e p —backing pressure.^f T —temperature for best fit.^g x —non-Boltzmann fraction.^h σ —standard deviation from experiment.

zle. The source was held at room temperature and the total backing pressure was about 1 atm. The rotational temperature of the pyrazine molecules in the beam was 2.5 K. In order to achieve MHz resolution the molecular beam was strongly collimated by two skimmers in a two step differential pumping system and spatially selective collection optics was applied. In the interaction zone, 30 cm downstream from the nozzle, the residual Doppler width was 15 MHz. The undispersed fluorescence was detected by a photomultiplier followed by a standard photon-counting system. The narrow band UV radiation was obtained by intracavity second harmonic generation in a modified Spectra Physics ring dye laser.^{10,11} A LiIO_3 angle tuned crystal was placed in the secondary waist of the cavity. About 2 mW of cw UV power with a bandwidth of less than 0.5 MHz was available.

III. OUTLINE OF THE CONTENTS

This section is intended to give a quick entrance to the various refinements of the theoretical interpretation necessary to be consistent with the measured excitation spectra, the invariance of the lifetime, the variation of the quantum yield across the rotational contour, and various other experimental results.

In Sec. IV we attempt to fit the J -resolved excitation spectra using simple symmetric top calculations. The agree-

ment with the experimental result is found to be very poor. In view of the variation of the quantum yield across the rotational contour, we look for a rotational dependence of the quantum yield.

In Sec. V we present high resolution excitation spectra of deuterated pyrazines, which suggest Coriolis coupling in the nonradiative decay. We assume an interstate Coriolis coupling in fitting the low-resolution spectra of pyrazine- h_4 , and we obtain considerable improvement. However, the fit is still not satisfactory for all temperatures.

We then show (Sec. VI) that for the lowest rotational temperature a non-Boltzmann distribution of the $J'' = 0$ ground state is likely, and good agreement is obtained with the experimental spectra.

In Sec. VII we actually calculate the variation of the quantum yield across the rotational contour, using the (known) interstate Coriolis coupling rate constants. Making use of the lifetimes of the ME's belonging to $P(1)$, we can calculate the absolute quantum yield of this rotational state which can then be used to estimate the absolute quantum yields of the other rotational states. This works for low J' , but for high J' our calculations drop off too fast with J' .

Thus, while interstate Coriolis coupling seems to be established, two problems arise:

(i) For large J' interstate Coriolis coupling between S_1 and S_0 yields a $1/J'^2$ dependence of the quantum yield, while

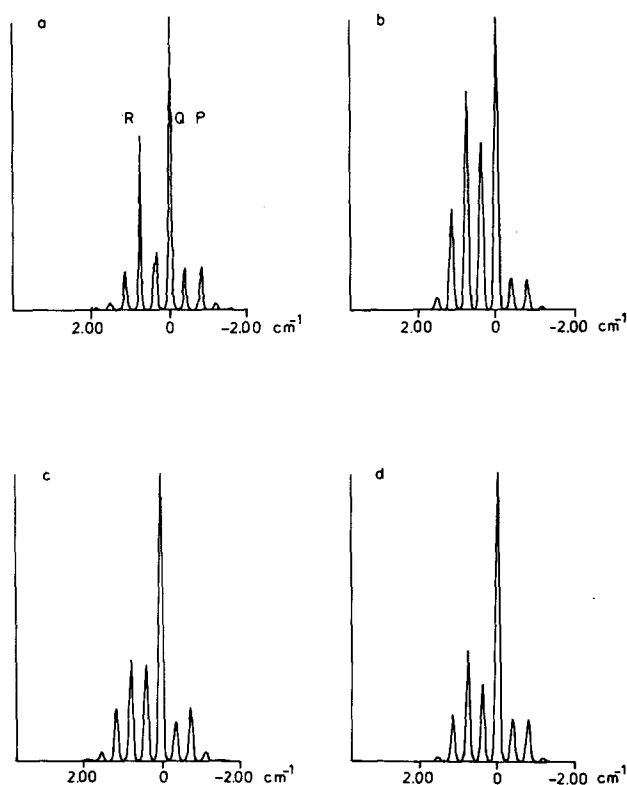


FIG. 1. (a) Experimental excitation spectrum, where excitation took place at 6 cm from the nozzle (stagnation pressure 2 bar of He). Note that the lines do not have the same width, their height is therefore misleading. (b) Calculated spectrum, using Eq. (3). (c) Calculated spectrum, assuming Coriolis coupling. (d) Calculated spectrum, assuming Coriolis coupling and non-Boltzmann distribution for $J'' = 0$.

a $1/J'$ dependence is observed⁷ and (ii) for large J' a systematic shortening of the lifetime of individual branches would then be expected [roughly (\propto) $1/J'^2$], while a constant lifetime is observed.

These problems can only be accounted for, when K scrambling¹² in the triplet manifold leads to an increased number of coupled triplet states, when $J' \geq 4$ (Sec. VIII). The quantum yield then will go as J'^{-1} , while the lifetime of the states is unaffected. We give reasons, why this coupling occurs only at higher J' 's.

K scrambling in the higher vibronic states of pyrimidine was actually observed by Nathanson and McLelland¹³ in fluorescence (de)polarization measurements. At 2025 cm^{-1} above the singlet origin the rotational motion was found to have a considerable statistical component. Taking into account the difference in singlet-triplet separation (4000 cm^{-1} for pyrazine and 2000 cm^{-1} for pyrimidine) one would also expect considerable vibration-rotation interaction in the triplet state of pyrazine at the energy of the singlet state.

IV. ANALYSIS OF THE LOW RESOLUTION SPECTRA IN THE SYMMETRIC TOP LIMIT

We have taken four low resolution excitation spectra of the ${}^1B_{3u}$ (0-0) transition of pyrazine under different conditions in the pulsed laser, free jet regime [see Fig. 1(a) and Table I]. They are labeled T_1 , T_2 , T_3 , and T_4 . We have reject-

ed the contribution of the fast component (which is considerable only in between the peaks), since it is either due to a very rapid (100 ps) dephasing¹⁴ or to nonresonant light scattering,¹⁵ which, using a nanosecond laser cannot be distinguished. The observed constancy of the lifetime¹⁶ permits the procedure of taking a constant time window for the integration of the emitted light to obtain the intensities of the excitation spectrum.

Throughout we will assume that the rotational spectrum is a parallel band,^{17,18} i.e., that there is no perpendicular contribution. At first we will describe the radiationless decay of pyrazine originating from a $S_1 - S_0$ internal conversion. The $T_1 - S_0$ intersystem crossing is assumed to be less probable, at least for the low J states. Towards the end, however, we will show that $T_1 - S_0$ relaxation must be included at higher J 's. Finally, we will assume that the supersonic nozzle yields a Boltzmann distribution, except where this is patently erroneous, as for the population of the $J'' = 0, K'' = 0$ state.

For a parallel band the fluorescence excitation intensities in the symmetric top approximation are given by

$$I_E(J'', K'' \rightarrow J', K') = (2J'' + 1) \cdot B_\Gamma \cdot g_\Gamma H(J'', K'' \rightarrow J', K') \cdot Y(J', K'), \quad (1)$$

where $I_E(J'', K'' \rightarrow J', K')$ is proportional to the emission intensity of the symmetric rotational state $|J', K'\rangle$ upon excitation of the transition $|J'', K''\rangle \rightarrow |J', K'\rangle$.

On the right-hand side of Eq. (1) $(2J'' + 1)$ is the M_J -degeneracy of $|J'', K''\rangle$, B_Γ the Boltzmann factor given by

$$B_\Gamma = \frac{\exp[-E(J'', K'')/kT]}{\sum_{J'', K''}^\Gamma (2J'' + 1) \exp[-E(J'', K'')/kT]}. \quad (2)$$

In Eq. (2) k is the Boltzmann constant, T the absolute temperature, and

$$E(J'', K'') = B'' J''(J'' + 1) + (C'' - B'')(K'')^2 \quad (3)$$

the energy of the oblate top ($C'' = 0.10249 \text{ cm}^{-1}$ and $B'' = 0.20526 \text{ cm}^{-1}$, the latter being the average of the asymmetric rotation constants²⁰ $A'' = 0.21285 \text{ cm}^{-1}$ and $B'' = 0.19767 \text{ cm}^{-1}$). The summation \sum^Γ in the denominator of Eq. (2) is restricted to those $|J'', K''\rangle$ states belonging to a particular irreducible representation Γ of the molecular point group D_{2h} of pyrazine.

In Eq. (1) g_Γ is the nuclear statistical weight¹⁹ given in Table II (note that by using these weight factors we fully account for the fact that pyrazine is actually not a symmetric top).

In Eq. (1) $H(J'', K'' \rightarrow J', K')$ are the Hoenl-London factors for a parallel band and its expressions are¹⁹

$$H(J'', K'' \rightarrow J'' + 1, K'') = \frac{(J'' + 1)^2 - K''^2}{(J'' + 1)(2J'' + 1)} \quad (4)$$

for the R branch and

$$H(J'', K'' \rightarrow J'', K'') = \frac{K''^2}{J''(J'' + 1)} \quad (5)$$

for the Q branch, and

$$H(J'', K'' \rightarrow J'' - 1, K'') = \frac{J''^2 - K''^2}{J''(2J'' + 1)} \quad (6)$$

for the *P* branch. Finally $Y(J',K')$ in Eq. (1) is the quantum yield of the upper $|J',K'\rangle$ state.

In applying Eq. (1) we first assume $Y(J',K') = Y$, i.e., independent of J',K' . The resulting best fit (T as the only parameter) for T_1 is shown in Fig. 1(b). Intensities expressed as a fraction of the total intensity are given in Table I (column *symm. top*), together with the best fit results for T_2 , T_3 , and T_4 . Obviously the agreement is poor, mismatches are in excess of 100%. It is of interest to note that this disagreement can hardly be due to the symmetric top approximation of Eq. (1) for reasons listed below:

(i) Since we do not experimentally resolve the K' states, the summation over all absorptions $\sum_{K',K''} I_A(J'',K'' \rightarrow J',K')$ is exact. This is also true if the $|J',K'\rangle$ states are coupled to a number of background states, simply because for any coupling the selection rule $\Delta J' = 0$ is strictly obeyed. Therefore, absorption intensity cannot be redistributed among different J' states.

(ii) A small error might arise in the calculations due to the asymmetric top transitions with $\Delta K = \pm 2$. The values of the rotational constants of pyrazine are such that for example the $\Delta K = 2$ transition of $R(2)$ has the same frequency as the $R(1)$ transition. However, calculations of asymmetric top intensities of $\Delta K = \pm 2$ transitions showed that the asymmetry of the rotor causes insignificant errors.

Thus, in conclusion, we can state that the calculation of the absorption through the Hoenl-London factors in Eq. (1) is very accurate (of course, only if the K' states are unresolved). We must therefore conclude that a J',K' independent quantum yield does not succeed in interpreting our data, as is also obvious from the results of Baba *et al.*^{8,9} and Amirav and Jortner.⁷ In the next section we therefore consider Coriolis coupling.

V. CORIOLIS COUPLING

A. General comments and deuterated pyrazines

The nonradiative decay rates due to Coriolis coupling between two singlet states have the form²¹

$$\Gamma_z = A_z^1 K'^2 \quad (K' \rightarrow K'), \quad (7)$$

$$\Gamma_+ = B_+^1 (J' - K')(J' + K' + 1) (K' \rightarrow K' + 1), \quad (8)$$

$$\Gamma_- = B_-^1 (J' + K')(J' - K' + 1) (K' \rightarrow K' - 1), \quad (9)$$

where A_z^1 , B_+^1 , and B_-^1 are constants to be obtained experimentally. The inspiration for using the above formulas comes from the *high resolution* spectra of pyrazine-*dh*₃ and pyrazine-*d*₃*h* shown in Fig. 2. These spectra taken with a resolution 200 times higher than those discussed in Sec. IV allowed us to investigate the fine structure within the rotational contours.

In case of pyrazine-*dh*₃ (Fig. 2, top) we observe the ME's belonging to the *P*(1), *P*(2), and the *Q* branch, which all have reasonable intensities. However, the transitions within *R*(0) are anomalously weak [note that *R*(0) and *P*(2) both terminate in $J' = 1$], while the *R*(1) is hardly observed. Even more anomalous is pyrazine-*d*₃*h* (Fig. 2, bottom) where *P*(1) is clearly observed, the intensities of the *P*(2) and the *Q* branch are weak, but no members of the *R* branch could be observed.

The main distinction between the two branches is that in the *R* branch the $|K'| = J'$ states cannot be excited. If these states have the highest quantum yield they will contribute most to the excitation spectrum and the *P* branch dominates. This will be the case if $A_z^1 < B_+^1, B_-^1$. A similar effect was found for channel III in benzene by Riedle, Neusser, and Schlag.²⁰

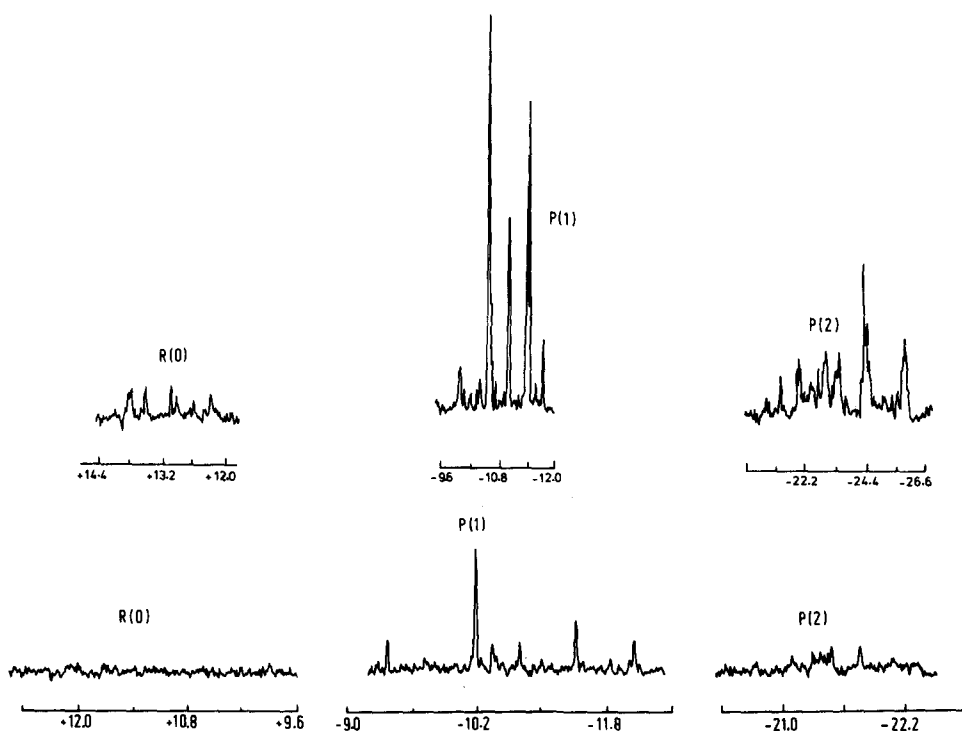


FIG. 2. Top: High resolution fluorescence excitation spectrum of pyrazine-*d*₃*h*₁ [the center frequency is at 30 999 573(18) cm^{-1}]. Bottom: High resolution fluorescence excitation spectrum of pyrazine-*d*₃*h*₁ [the center frequency is at 30 941(30) cm^{-1}]. Note that the *Q* branch is very weak. In addition, the *Q* branch is here very broad and structureless, and extends into the *P*(1). The frequency scales are in GHz.

For pyrazine- h_4 the effect is not immediately clear, but a close inspection of Figs. 1(a) and 1(b) also yields the conclusion that the P branch is generally relatively strong in relation to the R branch when compared to the calculated values. We will therefore incorporate the effect of Coriolis coupling on the excitation spectra.

Using Eq. (7) to Eq. (9) we have for the quantum yield $Y(J',K')$:

$$Y(J',K') = \frac{\Gamma_r}{\Gamma} \frac{1}{1 + A_z K'^2 + B_+(J' - K')(J' + K' + 1) + B_-(J' + K')(J' - K' + 1)}, \quad (12)$$

where $A_z = A_z^1/\Gamma$, $B_+ = B_+^1/\Gamma$, and $B_- = B_-^1/\Gamma$. Note that the factor Γ_r/Γ is a scaling factor in Eq. (1), and cannot be obtained from a fit of the excitation spectra.

It might be noteworthy that factoring Γ_r/Γ constitutes no approximation. However, the explicit (J',K') dependence in Eq. (12) depends on the "goodness" of the K' quantum number in the S_1 state. Figure 1(c) and Table I (column Cor) show the best fit using Eq. (12) for the quantum yield. It is seen that the improvement is very substantial (mismatches are now less than $\sim 30\%$). The values obtained for A_z^1 , B_+^1 , and B_-^1 of Eqs. (7)–(9) are

$$\begin{aligned} A_z^1 &= (0.2 \pm 0.1)\Gamma, \\ B_+^1 &= (0.25 \pm 0.05)\Gamma, \\ B_-^1 &= (0.05 \pm 0.05)\Gamma, \end{aligned}$$

which were used in further calculations.

Still, the fit is not satisfactory. Particularly, the calculated value of $R(0)$ is systematically too high, while $R(1)$ is calculated (systematically) too low (we have already mentioned that this cannot be explained by the asymmetric top $\Delta K = 2$ transitions of the Q branch). $R(0)$ arises from $J'' = 0$, $K'' = 0$ and apparently the calculation overestimates the population of this state, while underestimating it for others. This may point to a non-Boltzmann distribution in the beam, which we explore in the next section.

VI. NON-BOLTZMANN DISTRIBUTION

We note from Table II that the lowest levels of the A_g manifold are $J'' = 0$ and $J'' = 2, K'' = 2$. As a consequence,

TABLE II. Nuclear statistical weights.

J states	K_c states ^a	Symmetry	Weight
0, 2, 4, ...	0, 2, 4, ...	A_g	17
	-2, -4, ...	B_{3g}	9
	1, 3, 5, ...	B_{1g}	13
	-1, -3, -5, ...	B_{2g}	9
1, 3, 5, ...	0	B_{3g}	9
	2, 4, ...	A_g	17
	-2, -4, ...	B_{3g}	9
	1, 3, ...	B_{1g}	13
	-1, -3, ...	B_{2g}	9

^a Axes convention: Pyrazine belongs to the molecular point group D_{2h} . The $N-N$ axis is z , the other axis in plane is y , and the axis perpendicular to the molecular plane is x .

$$Y(J',K') = \frac{\Gamma_r}{\Gamma(J',K')}. \quad (10)$$

Writing

$$\Gamma(J',K') = \Gamma \left(1 + \frac{\Gamma_z}{\Gamma} + \frac{\Gamma_+}{\Gamma} + \frac{\Gamma_-}{\Gamma} \right), \quad (11)$$

where $\Gamma = \Gamma_r + \Gamma_{nr}$ is the decay rate constant of $J' = 0$, Eq. (10) can be rewritten as

establishing a Boltzmann distribution at low temperatures requires $\Delta J'' = -2$ collisions, and it is well known²² that the cross sections for $|\Delta J''| = 2$ collisions are in general less than $|\Delta J''| = 1$ collisions. Therefore, it is very possible that at low temperatures a Boltzmann distribution cannot be reached in the A_g manifold (note that for all other states, except the $J'' = 0$ state, $\Delta J'' = -1$ collisions are sufficient).

We can test this idea quantitatively by creating a fifth A_g "manifold," which consists of the $J'' = 0$ only, and has a population fraction x . The remaining part of the A_g manifold (denoted $A_g^{(1-x)}$) has a population fraction $(1-x)$. The nuclear statistical weights are of course the same for these two manifolds. We further assume that in the manifold $A_g^{(1-x)}$ Boltzmann equilibrium is reached. Note that the reference energy of the $A_g^{(1-x)}$ manifold is now $E(J'' = 2, K'' = +2)$. Figure 1(d) (and Table I, column Cor $N-B$) show the result, and the agreement with the experiment is now satisfactory, the misfit is now "delocalized" over all peaks, and below 20%. We emphasize that the only adjustable parameters used in obtaining Fig. 1(d) are the temperature T , and the population fraction x (we did not change the Coriolis coupling constants any further).

We finally mention that the kinetics of the $\Delta J'' = -2$ bottleneck depends on numerous factors like collisional partner and collisional frequency (the latter depends in turn on stagnation pressure, nozzle geometry, and so on). Therefore, for higher temperatures (T_3 and T_4), Boltzmann equilibrium for the A_g manifold can certainly be obtained, as is obvious from Table I.

VII. CALCULATION OF THE ABSOLUTE QUANTUM YIELD

Having obtained the Coriolis coupling constants A_z , B_+ , B_- we can calculate the relative quantum yield across the whole rotational contour, also for higher temperatures and compare our results with those of Amirav⁷ and Baba.^{8,9} To this purpose we calculate the absorption spectrum with the Hoenl-London factors and $Y = 1$ and the excitation spectrum with Y according to the Coriolis coupling and divide them point by point into one another. The width of the exciting light source leads to a certain averaging, which we mimic by giving every transition of the excitation and absorption spectrum a Gaussian width, comparable to the bandwidth of the light source. It should be noted that the latter procedure leads to a considerable lowering of the peak

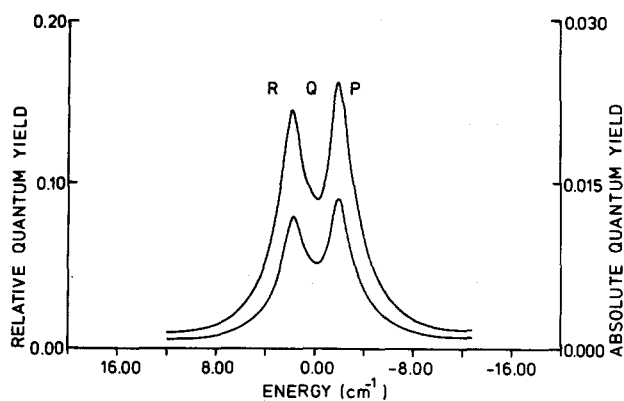


FIG. 3. The variation of the quantum yield across the rotational contour ($T = 20$ K) as calculated for an excitation bandwidth of 0.8 cm^{-1} for the minimum (upper trace) and maximum (lower trace) values of the Coriolis coupling rate constants. The left-hand axis gives relative values, the right-hand axis absolute values. The calculation should be correct for low J' (cf. Ref. 7).

value of the quantum yield, because of the strong dependence of the quantum yield on J' .

We show the results of these calculations in Figs. 3 and 4 for 20 and 300 K, respectively. They compare favorably with the measurements of Amirav and Jortner⁷ and with those of Baba *et al.*^{8,9}

To turn the relative quantum yield values into absolute ones we need a value for the quantum yield of the $P(1)$ transition, the state $J' = 0, K' = 0$ not being affected by Coriolis coupling.

The high resolution technique was used recently by Meerts *et al.* to measure the lifetimes of a number of individ-

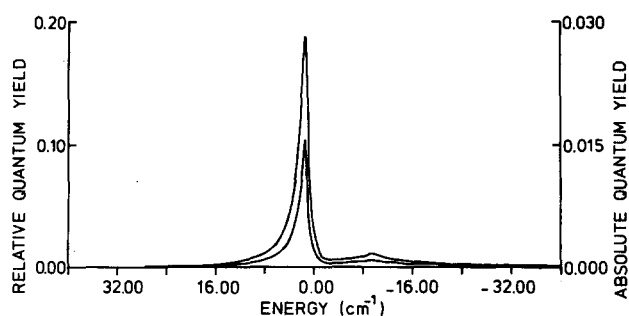


FIG. 4. As Fig. 3, but for $T = 300$ K and an excitation bandwidth of 0.5 cm^{-1} , again correct for low J' (cf. Refs. 8 and 9).

ual ME's within the $P(1)$ transition. The details will be published elsewhere, but the results are summarized here, since they allow a quantitative calculation of the absolute quantum yield of $P(1)$. Meerts' measurements unequivocally show there is radiationless decay of the zero-order triplet states, as well as of the singlet state. Table III summarizes both the measurements and the results of the deconvolution into zero-order states for the eight most important ME's.

Also, we determined the radiative lifetime of pyrazine from absorption measurements of a pyrazine solution to be about 290 ns, others have previously found 210 and 450 ns.^{23,24}

All these numbers can be introduced into the well-known equation²⁵ for radiationless decay for the coupling of one singlet (ω_s) to a number of triplets ω_T , which in their turn are coupled to a continuum. The singlet itself is also coupled to a continuum. Taking a "white" laser this equation is

$$C_S(\omega) = \frac{\Gamma_r/2\pi}{\omega - \omega_S - \sum_T (v_{ST}^2/\omega - \omega_T + i\gamma_T) + i(\Gamma_r^S + \Gamma_{nr}^S)}, \quad (13)$$

where Γ_{nr}^S denotes the width of $|S_1\rangle$ due to the coupling of the singlet to $\{S_0\}$ and γ_T the width of the triplets $\{T\}$ due to the coupling of the triplets to other states of $\{S_0\}$. The absorption is given by $\sum_i \Gamma_r |C_S^i|^2$, where i numbers the ME's, which if we use a white laser of course is equal to Γ_r . The emission can be found by Fourier transforming $C_S(\omega)$ to $\hat{C}_S(t)$ and then integrating $\Gamma_r |\hat{C}_S(t)|^2$. Dividing the calculated emission by the calculated absorption leads to the quantum yield for excitation with a light source broader than the spread of the ME's.

Using the values given in Table III we find $Q[P(1)] \approx 0.15$. Multiplying the relative quantum yield numbers with this quantity yields the absolute quantum yield, which in Figs. 3 and 4 are entered on the right-hand axes. For the peak value of Q we then find about 2% for the absolute quantum yield, which is in good agreement with the estimate made by Amirav and Jortner.⁷ A few remarks are now in order:

(i) The high resolution spectra of Meerts *et al.*⁴ showed 36 transitions which belong to the $P(1)$ contour. Only 8 were strong enough to measure their lifetimes. However, if

all the other 24 transitions are included the quantum yield decreases to 0.09, which is acceptable.

(ii) It should also be noted that the quantum yield given here holds for the whole singlet, i.e., for excitation with a white source. Clearly, if one would probe with a narrow laser the individual ME's, their quantum yields would differ considerably, since both their radiative and nonradiative life-

TABLE III. Energies, coupling elements, and decay rates of eight zero-order states of the ${}^1B_{3u}(0-0)$ $J' = 0, K' = 0$ state of pyrazine.^a

	Energy (MHz)	v_{ST} (MHz)	Γ_T (MHz)
Singlet	0		5 ± 4
	-1243	462	5 ± 1
	-459	119	1.6 ± 0.5
	-265	105	1.6 ± 0.7
Triplets	-55	150	2.7 ± 0.5
	+56	117	0.6 ± 0.5
	+516	457	3 ± 2
	+891	67	1 ± 0.5

^aFrom Ref. 4.

times vary considerably. In essence this is no more surprising than finding different quantum yields for different singlet states.

We have only one problem left. Careful comparison of the experimental data⁷ with the Coriolis calculation of the dependence of the quantum yield on the rotational contour shows that our calculated values drop off too fast with J' , particularly for higher J' values ($J' > 4$). We discuss this point in the next section.

VIII. THE NUMBER OF TRIPLETS COUPLED

As pointed out before us by Amirav and Jortner,⁷ the dropoff of the quantum yield with $(2J' + 1)$, as observed in their experiments, can easily be explained by assuming the number of triplets coupled to increase with $(2J' + 1)$. This could find its cause in K scrambling in the triplet manifold. Each J' , K' singlet can in principle couple with all states having a K' component. Since there are $(2J' + 1)$ of such states for each J' , very soon the decay would be totally determined by the triplet character of the ME's. However, because of the nuclear symmetry and the Pauli principle, the number should increase proportional to $1/4(2J' + 1)$, and in addition the triplets should display decay independent of J' . The latter assumption is bolstered up by calculations of Novak and Rice,²⁶ who showed that Coriolis coupling of triplet states is expected to be very small. The supposed increase in triplet coupling would also explain the constancy of the lifetimes with J' , as was observed by Lim *et al.*¹⁶ Apart from Coriolis coupling there appears to be no other J' , K' dependent mechanism for triplet decay, and although we would expect the radiationless lifetimes of the individual triplets to vary,⁴ on average they would yield a constant value.

This coupling through K scrambling can, however, not work for low J' , because of symmetry reasons. Of course, the $J' = 0$ state has only one K' , and K mixing is impossible. $J' = 1$ has three K' states, but since they are all of different symmetry, they cannot mix. $J' = 2$ has five K' states, but only two can mix; in $J' = 3$ one has seven states of which two pairs can mix, etc. We will find the onset of K scrambling for $J' \geq 4$. Our measurements of intensities depend heavily on the $J' < 4$ states, and there it appears that singlet-singlet Coriolis coupling dominates.

IX. CONCLUSIONS

From the high resolution spectra of the deuterated pyrazines clear evidence was found for the existence of a K dependence of the decay rates in the S_1 state. It was proposed that the mechanism responsible originates in a Coriolis coupling.

If we assume that Coriolis coupling between S_1 and $\{S_0\}$ is active in pyrazine h_4 as well, we can satisfactorily explain

the relative quantum yields of the J' states of the ${}^1B_{3u}$ (0-0) state of pyrazine for low J' . Lifetime measurements of the ME's belonging to the $J' = 0, K' = 0$ state show that zero-order triplet decay (independent of J', K') is also present. For $J' > 4$, the triplet decay starts to dominate because for these J' values K scrambling occurs. This effect accounts for the fact that the lifetime becomes constant for higher J' states.

Finally, in the course of our experiments we noticed a deviation from equilibrium for the lowest temperatures, probably caused by a bottleneck for $\Delta J = -2$ transitions.

ACKNOWLEDGMENTS

We gratefully acknowledge Willy Schutte for determining the radiative lifetime, and Dr. H. Th. Jonkman for his help in writing part of the computer program. Part of the research has been supported by the Foundation for Chemical Research (SON) with financial aid from the Netherlands Organization for Pure Research (ZWO).

- ¹B. J. van der Meer, H. Th. Jonkman, G. M. ter Horst, and J. Kommandeur, *J. Chem. Phys.* **76**, 2099 (1982).
- ²S. Okajima, H. Saigusa, and E. C. Lim, *J. Chem. Phys.* **76**, 2096 (1982).
- ³B. J. van der Meer, H. Th. Jonkman, J. Kommandeur, W. L. Meerts, and W. A. Majewski, *Chem. Phys. Lett.* **92**, 565 (1982).
- ⁴W. M. van Herpen, W. L. Meerts, K. E. Drabe and J. Kommandeur (to be published).
- ⁵B. J. van der Meer, H. Th. Jonkman, and J. Kommandeur, *Laser Chem.* **2**, 77 (1983).
- ⁶W. D. Lawrance and A. E. W. Knight, *J. Phys. Chem.* **89**, 917 (1985).
- ⁷A. Amirav and J. Jortner, *J. Chem. Phys.* **84**, 1500 (1986).
- ⁸H. Baba, U. Fujita, and K. Kekida, *Chem. Phys. Lett.* **73**, 425 (1980).
- ⁹H. Baba, N. Ohta, O. Sekicku, M. Fujita, and K. Kekida, *J. Phys. Chem.* **87**, 943 (1983).
- ¹⁰W. Majewski and W. L. Meerts, *J. Mol. Spectrosc.* **104**, 271 (1984).
- ¹¹W. Majewski, *Opt. Commun.* **45**, 201 (1983).
- ¹²D. B. McDonald, G. R. Fleming, and S. A. Rice, *Chem. Phys.* **60**, 335 (1981); Y. Matsumoto, L. H. Spangler, and D. W. Pratt, *Chem. Phys. Lett.* **98**, 333 (1983).
- ¹³G. M. Nathanson and G. M. McClelland, *J. Chem. Phys.* **84**, 3170 (1986).
- ¹⁴P. J. de Lange, K. E. Drabe, and J. Kommandeur, *J. Chem. Phys.* **84**, 538 (1986).
- ¹⁵H. Th. Jonkman, K. E. Drabe, and J. Kommandeur, *Chem. Phys. Lett.* **116**, 357 (1985).
- ¹⁶H. Saigusa and E. C. Lim, *J. Chem. Phys.* **78**, 91 (1983).
- ¹⁷J. A. Murit and K. K. Innes, *Spectrochim. Acta* **16**, 945 (1980).
- ¹⁸K. K. Innes, A. H. Kalantar, A. Y. Khan, and T. J. Durnick, *J. Mol. Spectrosc.* **43**, 477 (1972).
- ¹⁹G. Herzberg, *Electronic Spectra and Electronic Structure of Polyatomic Molecules* (Van Nostrand, Princeton, 1966).
- ²⁰E. Riedle, H. J. Neusser, and E. W. Schlag, *Faraday Discuss. Chem. Soc.* **75**, 387 (1983).
- ²¹E. Riedle, H. J. Neusser, E. W. Schlag, and S. H. Lin, *J. Phys. Chem.* **88**, 198 (1984).
- ²²T. Oka, *Adv. Atom Mol. Phys.* **9**, 127 (1973).
- ²³K. Nakamura, *J. Am. Chem. Soc.* **93**, 3138 (1971).
- ²⁴K. K. Innes, J. P. Byrne, and I. G. Ross, *J. Mol. Spectrosc.* **12**, 125 (1967).
- ²⁵R. Voltz, *Mol. Phys.* **19**, 881 (1970).
- ²⁶F. A. Novak and S. A. Rice, *J. Chem. Phys.* **73**, 858 (1980).